Progress of statistical modelling of thermal transport of fusion plasmas

メタデータ	言語: eng
	出版者:
	公開日: 2021-12-21
	キーワード (Ja):
	キーワード (En):
	作成者: YOKOYAMA, Masayuki, Yamaguchi, Hiroyuki
	メールアドレス:
	所属:
URL	http://hdl.handle.net/10655/00012795

Progress of statistical modelling of thermal transport of fusion plasmas

[1,2]M. Yokoyama and [1]H. Yamaguchi

[1]National Institute for Fusion Science, National Institutes of Natural Sciences, 322-6 Oroshi, Toki 509-5292, Japan

[2]The Graduate University for Advanced Studies, SOKENDAI, 322-6 Oroshi, Toki 509-5292, Japan

Abstract

Progress of statistical modelling of thermal transport of fusion plasmas based on a transport analysis database is described. Statistically induced ion and electron thermal diffusivities are checked with an actual discharge which had not been included in the database. Usefulness of this statistical approach is explained in terms of (1) extracting important parameters through the application of information criterion, and (2) making possible for discussing exponents of regression expression and then implying the thermal transport property. The statistical approach reported in this paper could provide a new insight for thermal transport modelling for fusion plasmas, complementing conventional global scalings on the energy confinement time.

1. Introduction

Statistical induction of a thermal transport model was proposed and found to be promising in Refs. [1-3] by exploiting transport analysis database for so-called "high ion-temperature discharge (hydrogen) scenario" (Fig. 2 of Ref. [2]) in the Large Helical Device (LHD) [4]. The integrated transport analysis suite, TASK3D-a [5], has been creating such transport analysis database.

After successful trials and increased recognition, the same approach was applied also to the electron channel (electron thermal transport) as an extension of preceding papers [1-3]. Furthermore, statistical extraction of important (contributing) variables with those radial variations for the thermal transport have been systematically performed. These investigations could increase the physics relevance (say, comparison to experimentally observed dependence) of the proposed statistical modelling.

It is strongly noted that actual numbers of regression expression in this paper are valid only within "LHD high ion-temperature discharge (hydrogen) scenario" database, and they are not directly applicable to any other experiments (even in the same device, LHD, with different discharge scenarios). This paper is intended to demonstrate reasonable feature and practicability of proposed statistical modelling of thermal transport, and to raise interests for performing similar approach in other

experiments. Furthermore, the obtained regression expression can be of a reasonable reference elucidating systematic dependence of thermal transport on plasma and configuration parameters.

This paper is organized as follows: The statistical induction of electron thermal transport (diffusivity) model is described in Sec. 2, to complement previously induced ion thermal transport model [2,3] Those relevance for reproduction of ion and electron thermal diffusivity, and then ion and electron temperature profiles was checked against actual LHD discharge which had not been included in a transport analysis database. In Sec. 3, exhaustive search with utilizing Akaike's Information Criterion (AIC) [6] is described to statistically extract important (contributing) parameters for thermal transport. It is also investigated how such important parameters and those exponents radially vary, which could elucidate the different characteristics of thermal transport according to radial positions. Finally, summary and discussion are provided in Sec. 4.

2. Descriptions on statistically induced thermal transport model and demonstration of its practicability

Here, essential points on how the statistical induction of thermal transport model has been developed are briefly explained. The integrated transport analysis suite, TASK3D-a [5], has accumulated power-balance analysis results for "high ion-temperature discharge (hydrogen) scenario" in LHD to provide ion and electron thermal diffusivity profiles. As an example, results of approximately total 200 timings (when all the density and temperature profiles are measured) from 31 discharges are compiled as a database for this study, which ends up about 3000 data points for ion and electron thermal diffusivity (with keeping radial profiles), respectively. This database is shown as Fig. 2 of Ref. [2]. The parameter ranges near the core region in this database are as summarized follows. The ion temperature (T_i) is from ~2 to ~7 keV, the electron temperature (T_e) is from ~2.5 to ~4 keV, and the electron density (n_e) is from ~1 to ~1.7 x 10^{19} m^{-3}. It is also noted here that the data for at the very core region (that is $r_{eff}/a_{99}<0.15$) are excluded (as shown in Fig. 2 of Ref. [2]) since rather low temperature and density gradient there increases the uncertainty for the evaluation of the thermal diffusivity). Here, r_{eff}/a_{99} is the averaged minor radius (equivalent simple torus) and a_{99} is the effective minor radius inside of which 99 % of the electron pressure exists [7]. These datapoints of thermal diffusivity are regressed based on *a priori* set nine explanatory variables (all normalized, and all local values) as listed in Table 1 of Ref. [2] (for ion data).

The regression expression for the normalized ion thermal diffusivity, $\frac{\chi_i}{r_{eff}^2 \omega_i}$, was reported in Refs.

[2,3] through log-linear multivariate regression analysis. The obtained expression is repeated below.

$$\frac{\chi_i}{r_{eff}^2 \omega_i} = 10^{-12.1} \nu_i^{*-0.28} \rho_i^{*-1.49} (T_e/T_i)^{0.54} (R/L_{Ti})^{-0.81} (R/L_{ne})^{0.014} (\iota/2\pi)^{0.55} \epsilon_h^{-0.88} \epsilon_t^{-1.98} \epsilon_{eff}^{0.71} \quad (1),$$

The electron channel ($\frac{\chi_e}{r_{eff}^2 \omega_e}$) was not considered there, since the range of the electron temperature in

the database was narrower than that of the ion temperature and thus originally thought that the regression property may be worse compared to that of ion channel. However, it happened to be found that similar set of explanatory variables (for electrons by replacing quantities for ions by those for electrons, based on Table 1 in Ref. [2]) resulted in higher coefficient of determination, R^2, as high as 0.98 with the regression expression,

$$\frac{\chi_e}{r_{\text{eff}}^2 \omega_e} = 10^{-15.4} \nu_e^{*-0.39} \rho_e^{*-0.59} (T_e/T_i)^{-0.22} (R/L_{Te})^{-0.49} (R/L_{ne})^{0.027} (\iota/2\pi)^{0.42} \epsilon_h^{-0.74} \epsilon_t^{-3.27} \epsilon_{\text{eff}}^{0.98} \quad (2).$$

The comparisons of $\log_{10}(\chi/r_{\text{eff}}^2 \omega)$ values between TASK3D-a analysis database and the regression results based on the above expressions are shown in Fig. 1 ((a) for ion [reproduction from Ref. [3]] for completeness, and (b) for electron).
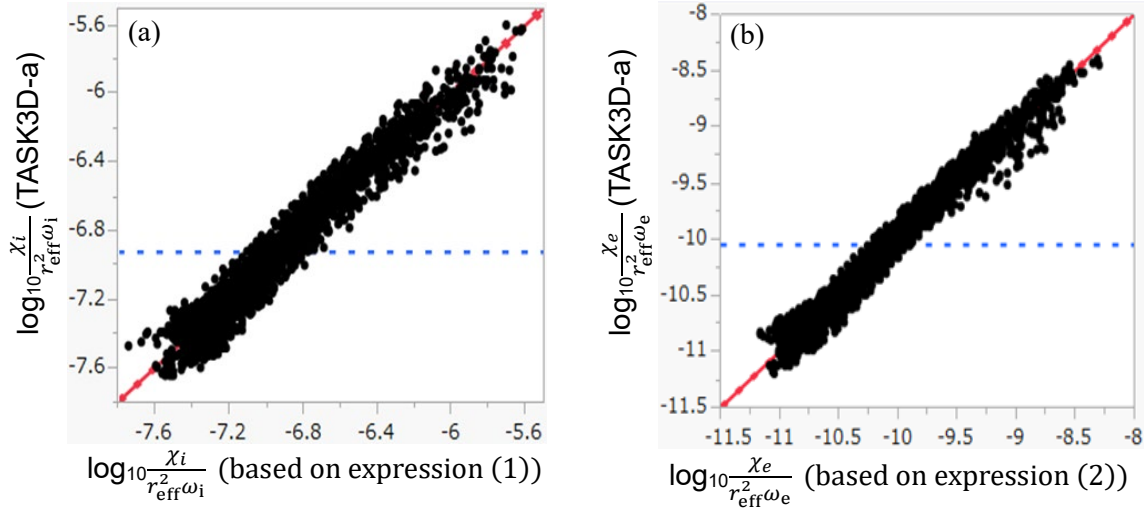

Fig.1 The comparison of (a) $\log_{10}\frac{\chi_i}{r_{\text{eff}}^2 \omega_i}$ and (b) $\log_{10}\frac{\chi_e}{r_{\text{eff}}^2 \omega_e}$ values between TASK3D-a analysis database and the regression expressions. (a) is reproduced from Fig. 4 in Ref. [3].

To check the practicability of the obtained regression expressions, the ion and electron thermal diffusivities, χ_i and χ_e, are evaluated with these expressions and then compared to the experimentally evaluated (TASK3D-a) ones. This is done for total of 12 timings (all with T_i measurement) of 2 discharges (6 each, shots of 109125 (3.94s – 4.44s) and 123130 (4.64s – 5.14s)) which had not been included in the analysis database, but with plasma parameters (density and temperatures) and magnetic configurations mostly within the range of the database. The shot 101925 is characterized as the evolution of T_i at the core region is small (about 3~4 keV), and 123130 is large (about 4 to ~7-8 keV).

It should be noted here that estimates by regression expressions are made only for radial region of $r_{\text{eff}}/a_{99}>0.15$ based on the radial range of the employed TASK3D-a analysis database. Figure 2 is shown as tabular setting for (upper) χ_i and (lower) χ_e by (left) TASK3D-a and (right) regression expressions (1) and (2), for these two discharges. It is seen that there are visible discrepancies, for example, χ_i for outer region of both discharges. However, TASK3D-a results and estimates by regression expressions (both χ_i and χ_e) match reasonably well each other in the inner radii region for most of the cases (except, 4.44s of 109125). As for χ_e, the trend that χ_e is more or less monotonically increasing towards the inner region is rather well reproduced. Thus, it is considered that the proposed statistical approach can reasonably reproduce the thermal diffusivity profiles for ion and electron simultaneously, with rather simple expressions as in (1) and (2). Of course, further improvement is demanded, in particular, for outer region, which might be pursued by expanding the analysis database to include wider temperature range there.

Further check is conducted by comparing ion and electron temperature profiles simulated with expressions (1) and (2) and the experimentally observed ones, as shown in Fig. 3 (tabular settings similarly as Fig. 2). In these simulations, the density profile is fixed as measured, NBI deposition profile is precalculated by TASK3D-a, and the heat diffusivity profiles (based on regression expressions) are fixed as those in Fig. 2. Since the regressed χ_i tend to be smaller than those of TASK3D-a at outer region for 109125 as shown in Fig. 2, the simulated ion temperature becomes larger at outer region, and then this feature is kept towards inner region to reach at most about 1 keV (~25 %) difference at the plasma core (for example, 4.24s of 109125). As for 123130, the temporal evolution of T_i at inner region (increasing from 4.64s to 4.74, 4.84s, and then decreasing afterwards) is rather well tracked, but maximum T_i (around 4.74s and 4.84s) associated with the increased gradient cannot be quantitatively reproduced. On the other hand, the electron temperature is rather well reproduced, except the one case, 4.64s of 123130. This apparent overestimate is due to the smallness of χ_e at the very close to the edge (visible in red at the figure of χ_e (regression result), which forms the steep temperature gradient there compared to the other cases. The temperature gradient at inner region for this case is almost similar to the other cases.

Based on these 12 cases of validity checks, it is concluded that the present regression expressions (1) and (2) are not the perfect ones. The trend such as temperature evolution can be reproduced to some extent, but systematic and quantitative reproduction (in particular, for T_i) has not been achieved. Although further trials on the statistical approaches should be required to increase the reproducibility of temperature profiles, the proposed statistical approach itself can be promising to "describe" the thermal transport property of fusion plasmas.

Shot 109125	TASK3D-a	Regression results

χi		
χe		

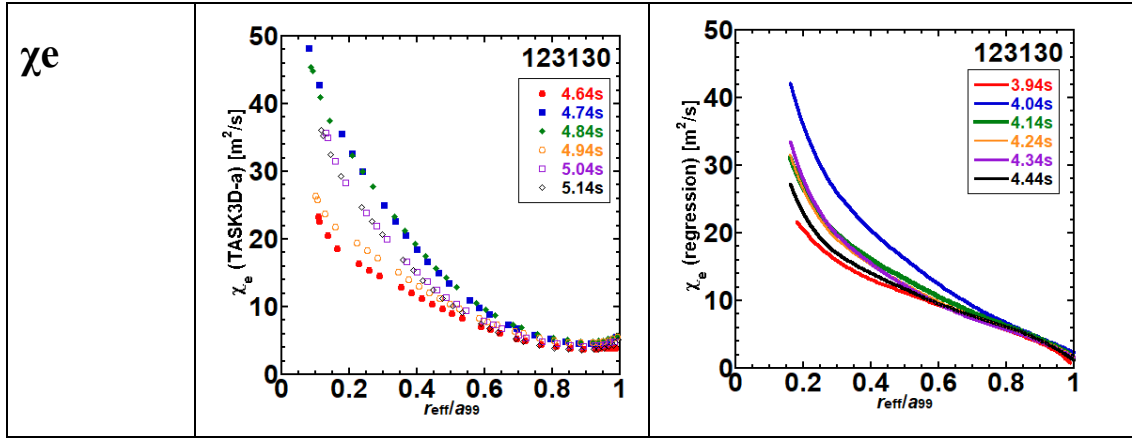| Shot 123130	TASK3D-a	Regression results
χi		

χe	
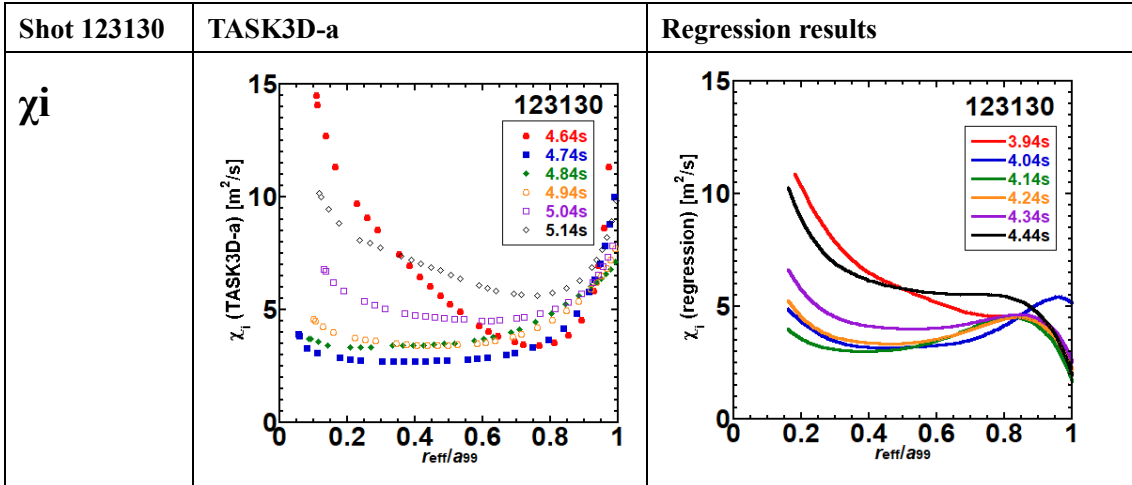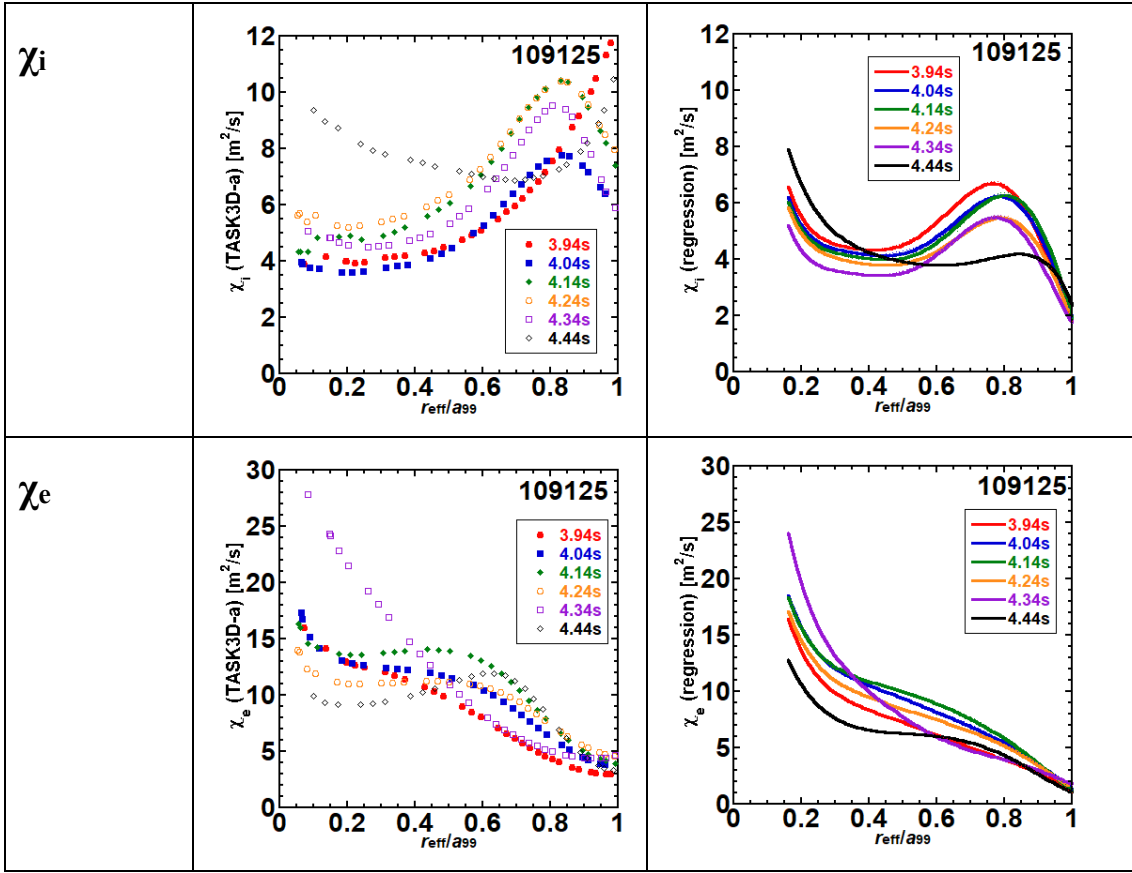
Fig. 2 The (upper) ion and (lower) electron thermal diffusivities, χ_i and χ_e for results by (left) TASK3D-a and (right) regression expressions (1) and (2), for these two discharges, 109125 and 123130.

Shot 109125	Experiment	Simulated by regressed thermal diffusivities
Ti		
Te		

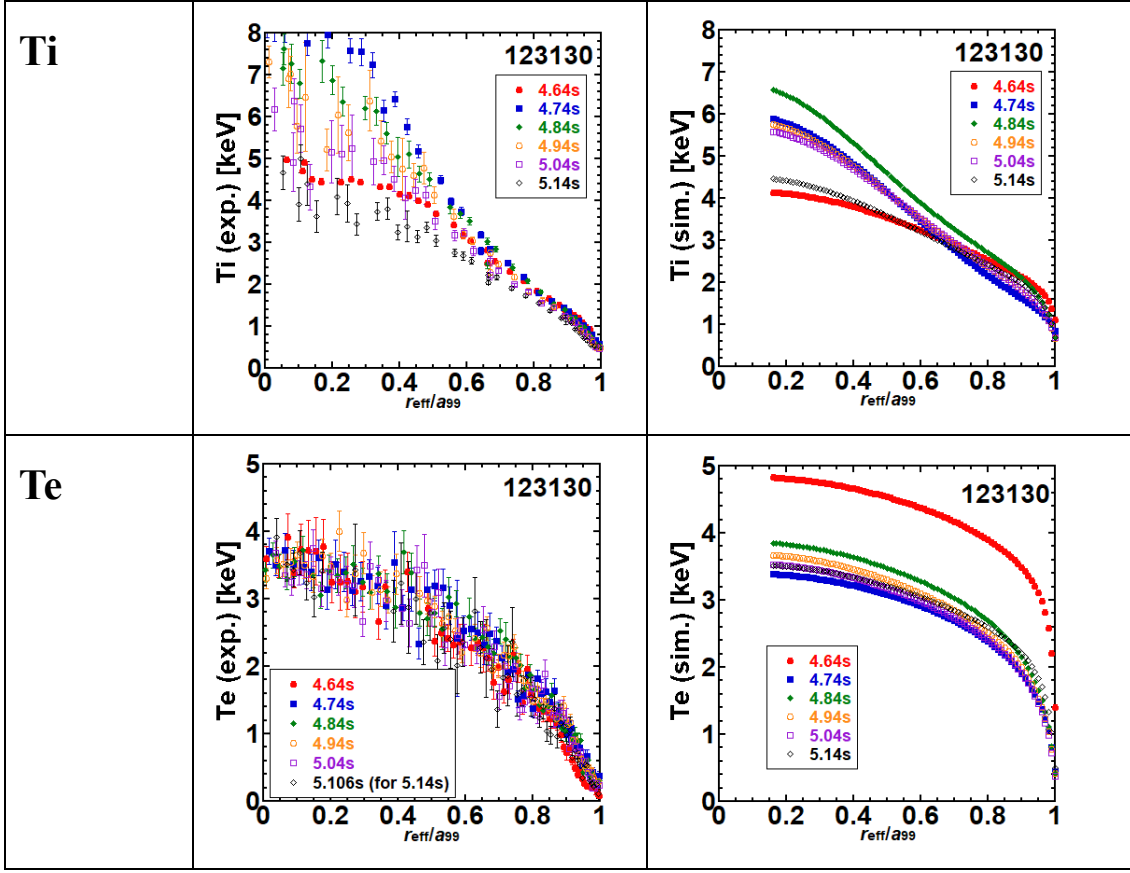| Shot 123130	Experiment	Simulated by regressed thermal diffusivities

Fig. 3 The (upper) ion and (lower) electron temperature profiles for (left) experimental observation and (right) simulated by regressed thermal diffusivities, for these two discharges, 109125 and 123130.

3.   Statistical analysis towards physics interpretations on the induced regression expressions

3.1 Statistical extraction of important parameters

In this section, other useful aspects of statistical modelling are described, based on utilization of the information criterion. In this paper, Akaike's information criterion (AIC) with correction for small sample sizes (AICc) [8] is continuously used based on the preceding Letter [2]. AIC is the measure for the relative quantity of statistical models for a given dataset. It is again noted here that Bayesian information criterion (BIC) [9] gives almost the same values as those of AICc for data size of O(3000) in this analysis.

The evolution of AICc was investigated by stepwise addition of each variable as seen in Fig. 5(b) in Ref. [3]. Here, as its extension, results for exhaustive investigation of AICc, along with R^2 at the lowest AICc, for all possible combinations of *a-priori* prepared 9 parameters (as listed in Table 1 in Ref. [2]) for the ion thermal diffusivity for $r_{eff}/a_{99}<0.35$ are shown in Fig. 4. The range of AICc values for each number of variables (NV) indicates that AICc vary within that range for different combinations with designated NV. In Fig. 4, open symbols correspond to that of expression (3) in Ref. [3] with 4 variables.

It was induced from the stepwise addition of variables (as Fig. 5(b) in Ref. [3]) and omitting one of strongly correlated variables. That combination is confirmed to reach almost minimum AICc among all possible combinations with NV=4. It is seen that AICc minimum steadily decreases up to NV=5, and then almost unchanged afterwards, as is the case for R^2. Thus, it is considered that the combination of 5 variables giving the minimum AICc corresponds to the "statistically" optimal model. Thus, the appearance of variables and those exponents up to NV=5 are summarized in Table 1. The R/L_{Ti} firstly appears (at NV=1) and keep appearing up to NV=5, which indicates that R/L_{Ti} is statistically important variable to regress the ion thermal diffusivity. The appearance of three variables related to magnetic configuration, ϵ_h, ϵ_t and $\iota/(2\pi)$, is not physically and intuitively interpreted in a straightforward manner (in particular, negative exponents of magnetic field ripples), but these variables contributes to reach minimum AICc in statistical viewpoints. It is noted that the current database is formulated with experiments performed on limited magnetic configurations (vacuum magnetic axis positions of 3.60 m and magnetic field strength of 2.75 – 2.85 T) for "high ion-temperature" scenario. Thus, the parameter range of these configuration-related variables are narrow compared to those of plasma parameters, and physics interpretation on configuration dependence may need to expand those parameter ranges. Other than configurational parameters, temperature ratio, T_e/T_i, and normalized ion Larmor radius, ρ_i^*, contributes lowering AICc from NV=3 and 4, respectively. It should be pointed out that exponents of R/L_{Ti}, T_e/T_i and ρ_i^* change the absolute values but keep the sign up to NV=5.

The same approach is applied to electron thermal diffusivity for $r_{eff}/a_{99}<0.35$, as plotted in Fig. 5. It is seen that AICc minimum is reached already at NV=4, and the corresponding variables and exponents are listed in Table 2. Similarly to a case for the ion thermal diffusivity, R/L_{Te} firstly appears, and ρ_e^* follows in addition to the configurational variables, ϵ_t and ϵ_{eff}. The exponents of R/L_{Te} and ρ_e^* keep their sign and converge more or less to about -1 and 5, respectively. On the other hand, for cases with the lowest AICc for each NV, T_e/T_i, appears at NV=7 at last, which indicates the contribution of the temperature ratio to "statistically" determine the electron thermal diffusivity is less than that to the ion thermal diffusivity. The T_e/T_i appears at the second lowest AICc at NV=4, for which its exponent is 0.15. This exponent is far below that for the ion thermal diffusivity (Table 1). The temperature ratio seems to affect the ion thermal diffusivity more than the electron diffusivity. In this way, AICc can be used to statistically extract responsible variables and those exponents to describe the thermal diffusivity of fusion plasmas, complementing the usual first-principle approach.
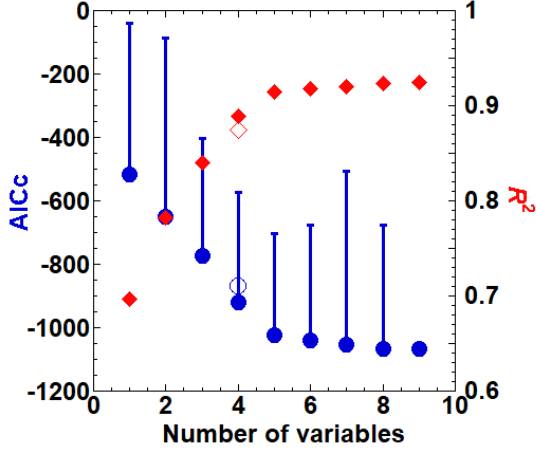
8

Fig. 4 The evolution of AICc values (solid circles with ranges) and R^2 (diamonds) for the ion thermal diffusivity for $r_{\text{eff}}/a_{99}<0.35$ as a function of number of variables (NV). Open symbols correspond to those in a case of the regression expression (3) in Ref. [3].

Table 1   Appearance of variables and those exponents as a function of number of variables up to NV=5 (at the lowest AICc for each NV) for the ion thermal diffusivity for $r_{\text{eff}}/a_{99}<0.35$.

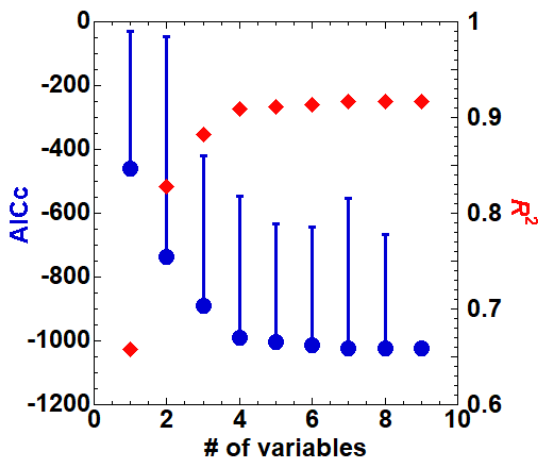| Number of variables	$\rho_i{}^*$	R/L_{Ti}	T_e/T_i	ϵ_h	ϵ_t	$\iota/(2\pi)$	AICc	R^2
1		-1.43					-516.6	0.696
2		-1.08			-1.00		-650.05	0.782
3		-0.92	0.55	-1.08			-772.83	0.840
4	3.64	-0.89	2.63		-1.06		-918.43	0.889
5	3.79	-0.84	2.88		-1.37	1.97	-1023.9	0.914

Fig. 5 The evolution of AICc values (solid circles with ranges) and R^2 (diamonds) for the electron thermal diffusivity for $r_{\text{eff}}/a_{99}<0.35$ as a function of number of variables (NV).

Table 2   Appearance of variables and those exponents as a function of number of variables up to NV=4 (at the lowest AICc for each NV) for the electron thermal diffusivity for $r_{\text{eff}}/a_{99}<0.35$.

Number of variables	$\rho_e{}^*$	R/L_{Te}	ϵ_t	ϵ_{eff}	AICc	R^2

9

1		-1.71			-460.37	0.658
2	5.70	-1.53			-737.65	0.828
3	6.16	-1.05	-0.90		-888.27	0.882
4	5.51	-1.15	-1.77	0.61	-991.24	0.909

3.2 Statistical investigation on exponents of important parameters and its implication to thermal transport property

In Sec. 3.1, the extraction of important parameters and those exponents based on the exploitation of AICc was described. Here in this subsection, radial variation of exponents is examined and then its implication to thermal transport property is discussed. For this purpose, let the important variables fixed to those discussed for $r_{eff}/a99<0.35$ ($\rho*$, T_e/T_i, R/L_T and ϵ_h) in the previous publication (expression 3) in Ref. [3], to systematically consider the radial variation of exponents without radial change of basis-variables. Indeed, the three parameters, $\rho*$, T_e/T_i and R/L_T, simultaneously appear for ion cases with the lowest AICc at NV=3 also for dataset for 0.4< $r_{eff}/a99$<0.6 and 0.7< $r_{eff}/a99$<0.9, respectively. Here, this subdivision into 3 radial regions is made to consider inner (inside ion internal transport barrier for high T_i phases), mid-radius, and close-to-edge regions with keeping enough data points in each region (404, 708 and 718 points, respectively). While, contribution of T_e/T_i on the electron thermal diffusivity is much less than that for ions, and it appears (for the lowest AICc minimum) at NV=7 for all radial regions. It is also noted that configurational variable, ϵ_h, is kept since its exclusion does increase AICc and reducing R^2.

Table 3 summarizes the exponents of these four variables for three different radial region, $r_{eff}/a99<0.35$ ~~(inner region)~~, 0.4< $r_{eff}/a99$<0.6~~(mid-radius)~~ and 0.7< $r_{eff}/a99$<0.9~~(outer region)~~ for (a) ion and (b) electron thermal diffusivity. The R^2 is also listed for each region.

Table 3   Exponents of 4 variables (as in the expression (3) in Ref. [3]) in the log-linear multivariate regression for (a) the ion and (b) the electron thermal diffusivities for three radial regions. along with corresponding R^2.

(a)

$r_{eff}/a99$	ρ_i*	T_e/T_i	R/L_{Ti}	ϵ_h	R^2
<0.35	2.79	2.32	-0.94	-0.58	0.87
0.4-0.6	2.15	2.08	-0.89	-0.43	0.7484
0.7-0.9	0.95	1.52	-0.62	-0.11	0.6467

(b)

$r_{eff}/a99$	ρ_e*	T_e/T_i	R/L_{Te}	ϵ_h	R^2

<0.35	5.85	0.27	-1.21	-0.39	0.87
0.4-0.6	4.41	0.24	-1.21	-0.048	0.87
0.7-0.9	3.99	0.21	-0.13	0.23	0.79

For illustration, comparisons of $\log_{10}\frac{\chi_i}{r_{\text{eff}}^2\omega_i}$ and (b) $\log_{10}\frac{\chi_e}{r_{\text{eff}}^2\omega_e}$ values between TASK3D-a analysis database and the regression results (Table 3) are shown in Figs. 6.
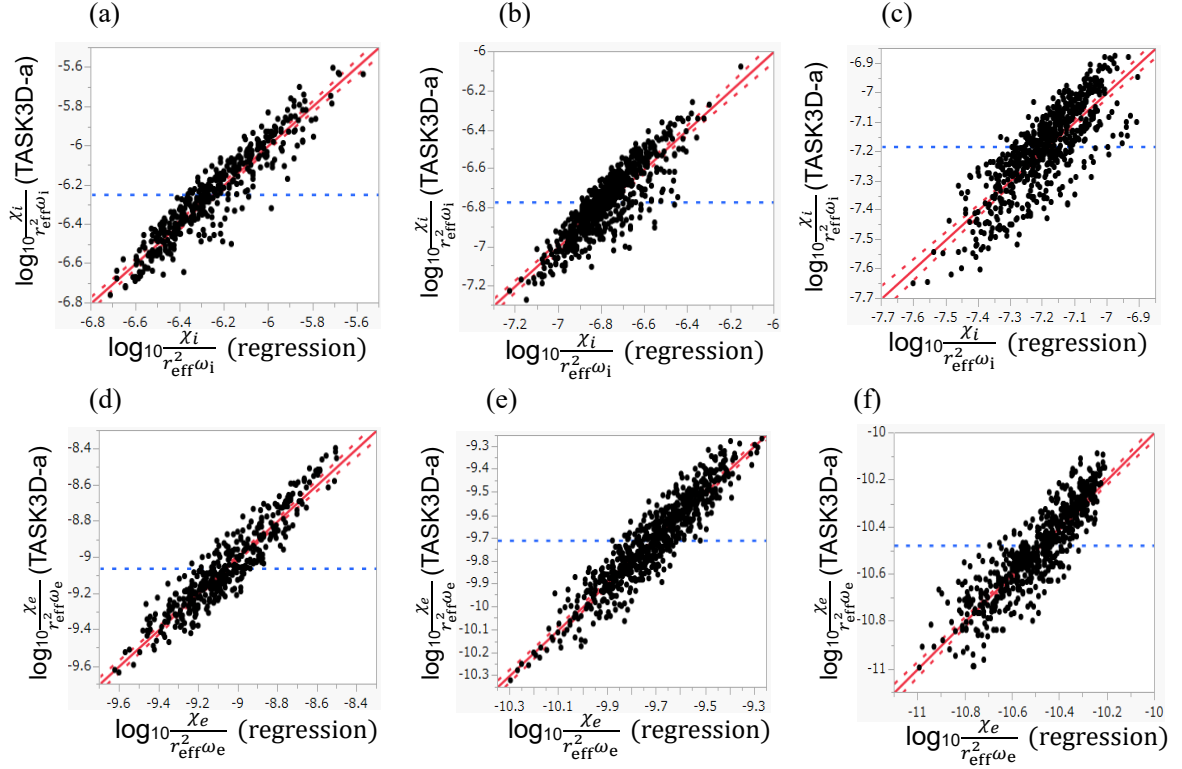

Fig.6 The comparisons of $\log_{10}\frac{\chi_i}{r_{\text{eff}}^2\omega_i}$ and $\log_{10}\frac{\chi_e}{r_{\text{eff}}^2\omega_e}$ values between TASK3D-a analysis database and the regression results (Table 3), (a)-(c) for ions, and (d)-(f) for electrons, from left to right, for $r_{\text{eff}}/a_{99}<0.35$, $0.4< r_{\text{eff}}/a_{99}<0.6$ and $0.7< r_{\text{eff}}/a_{99}<0.9$, respectively. (a) is reproduced from Fig. 6(d) in Ref. [3].

The R^2 decreases from inner to outer region. However, it keeps larger than 0.6 (for the ion thermal diffusivity for $0.7<r_{\text{eff}}/a_{99}<0.9$), which can be considered that the model with these four variables is still statistically relevant, as seen in Fig. 6(c). The exponents of ρ^* are larger for electrons than those for ions, and they are decreasing towards outer region for both ions and electrons. Contrary to this, exponents of T_e/T_i are larger for ions, and they are decreasing towards outer region. The exponents of R/L_T keep negative value and tend to become smaller in the absolute value towards outer region. The

immediate physics interpretation and understanding cannot be withdrawn from Table 3.

For transport analyses of LHD plasmas, neoclassical and turbulent transport simulations have been extensively conducted such as by GSRAKE (solving the ripple-averaged kinetic equation) [10], FORTEC-3D (solving the drift kinetic equation based on the δf Monte-Carlo method) [11], and GKV (solving the gyrokinetic Vlasov equation) [12], respectively, all of which have been developed to deal with three-dimensional magnetic configurations. The code applications have been done mostly for case-by-case basis. It has come to the stage that the ion thermal transport for high ion-temperature plasma can be quantitively reproduced by combination of these large-scale simulation results [13]. However, this has been done for a small number of cases, and thus concrete parameter dependence as described in expressions (1) and (2) has not been obtained. Thus, this kind of comparisons (Table 3) with multivariate variables, between ions and electrons, and between radial regions, may resolve complicated entanglements between these variables to describe the thermal transport property. Then, it provides reasonable guidance for identifying and inducing relevant physics models and performing large-scale simulations.

As for comparison to experimental findings of LHD (high ion-temperature scenario), the negative-power dependence of the ion thermal diffusivity on R/L_{T_i} has been confirmed (at $r_{eff}/a_{99}=0.3$ and 0.5) in Ref. [14], and its positive-power dependence on T_e/T_i has also been confirmed (at $r_{eff}/a_{99}=0.31$ and 0.98) in Ref. [15]. It should be worthwhile to examine how the experimentally identified trends of thermal diffusivities can be grasped based on this multivariate regression approach. This will be performed in a separate paper.

4.　Summary and Discussion

Progress of statistical modelling of thermal transport of fusion plasmas are described after previous publications, by utilizing the same transport analysis database ("high ion-temperature discharge (hydrogen) scenario" of LHD).

As a complement, the log-linear multivariate regression result for the normalized electron thermal diffusivity is obtained. Along with that for ion [3], the promising practicability of the ion and electron thermal diffusivity (with radial profiles) is confirmed for the LHD discharge which had not been included in the database.

It is also noted here that this statistical approach can provide reasonable initial guess of transport models for conducting data assimilation [16] in which the transport models are updated and optimized to align the simulation results to experimentally measured values (such as temperatures).

Useful aspects of statistical modeling are also explained; the one is the statistical extraction of important parameters, and the other is the statistical investigation on exponents of important parameters and then its implication to thermal transport property. The former is performed by consideration of information criterion (AICc in this paper). It is found that certain parameters which

seem to be important to describe the thermal diffusivity are naturally extracted (with its exponents in multivariate regression expression) through the exhaustive investigation of AICc. Parameters are prepared, *a priori*, in this paper, but one can prepare parameters according to own physics interests, and then specify how those parameters are quantitatively "important" in order by this approach. The latter can provide quantitative comparison of exponents of important variables, between ion and electron, and between radial regions. This may resolve complicated entanglements between physics variables to describe thermal transport property and lead a reasonable guidance for identifying relevant physics models.

After this paper, transport analysis database for other heating scenarios in LHD, and even that for other fusion experiments will be examined based on the proposed statistical approach. This could provide a new insight for thermal transport modelling for fusion plasmas, complementing global scalings.

References

[1] M. Yokoyama and H. Yamaguchi, Plasma Fusion Res. **14** (2019) 1303095.

[2] M. Yokoyama, Nucl. Fusion **59** (2019) 094004.

[3] M. Yokoyama, Nucl. Fusion **60** (2020) 029501 (Corrigendum to Ref. [2]).

[4] Y. Takeiri et al., Nucl. Fusion **57** (2017) 102023.

[5] M. Yokoyama et al., Nucl. Fusion **57** (2017) 126016.

[6] H. Akaike, "Information theory and an extension of the maximum likelihood principle", Proceedings of the 2nd International Symposium on Information Theory, Petrov, B. N., and Caski, F. (eds.), Akadimiai Kiado, Budapest (1973) 267.

[7] C. Suzuki et al., Plasma Phys. Control. Fusion **55** (2013) 014016.

[8] N. Sugiura, Communications in Statistics - Theory and Methods **7** (1978) 13.

[9] G. Schwarz, The Annals of Statistics **6** (1978) 461.

[10] C. D. Beidler and W. N. G. Hitchon, Plasma Phys. Contr. Fusion **36** (1994) 317.

[11] S. Satake et al., Plasma Fusion Res. **1** (2006) 002.

[12] T-H. Watanabe et al., Nucl. Fusion **46** (2006) 24.

[13] M. Nunami et al., Plasma Phys. **19** (2012) 042504.

[14] K. Nagaoka et al., Nucl. Fusion **59** (2019) 100602.

[15] H. Takahashi et al., Nucl. Fusion **57** (2017) 086029.

[16] Y. Morishita et al., Nucl. Fusion **60** (2020) 056001.